Available online at www.sciencedirect.com
SCIENCE DIRECT
Polymer 46 (2005) 8926–8936
polymer
www.elsevier.com/locate/polymer

Plastic deformation of polyethylene crystals as a function of crystal thickness and compression rate

T. Kazmierczak[a], A. Galeski[a,*], A.S. Argon[b]

[a]*Centre of Molecular and Macromolecular Studies, Polish Academy of Sciences, Sienkiewicza 112, 90-363 Lodz, Poland*
[b]*Mechanical Engineering Department, Massachusetts Institute of Technology, Cambridge, MA 02139, USA*

Received 25 January 2005; received in revised form 24 June 2005; accepted 27 June 2005
Available online 3 August 2005

Abstract

Plastic deformation of polyethylene (PE) samples with crystals of various thickness was studied during uniaxial compression with initial compressive strain rates of 5.5×10^{-5}, 1.1×10^{-3} and 5.5×10^{-3} s^{-1}. Samples with a broad range of crystals thickness, from usual 20 up to 170 nm, were obtained by crystallization under high pressure. The samples underwent recoverable compression below the compression ratio of 1.05–1.07. Following yield, plastic flow sets in above a compression ratio of 1.12. At a compression rate of 5.5×10^{-5} s^{-1} the yield stress increases with the increase of crystal thickness up to 40 nm. For crystals thicker than 40 nm the yield stress levels off and remains constant. This experimental dependence was compared with the model developed on the basis of classical crystal plasticity and the monolithic nucleation of screw dislocations from polymer crystals. In that model contrary to the experimental evidence, the yield stress does not saturate with increase of crystal thickness. The activation volumes determined from strain rate jump experiments and from stress relaxation for crystals thicker than 40 nm are nearly constant at a level of 8.1 nm^3. This activation length agrees very well with 40 nm for crystal thickness above which the yield stress levels off. It is proposed, as shown in a companion communication, that for PE crystals thicker than 40 nm two other modes of dislocation emission in the form of half loops of edge and screw dislocations begin to govern the strain rate, which no longer depend on lamella thickness.

Keywords: Yield stress; Crystal thickness; Polyethylene

1. Introduction

There are still unexplored areas concerning plastic deformation of crystalline polymers. The elastic part of the deformation can be almost entirely attributed to the reversible interlamellar shear. However, the yield and the plastic flow that follows are often obscured by cavitation [1]. For the yield behavior of semi-crystalline polymers there have been two conflicting considerations. In the first, the process of deformation is attributed to a simultaneous melting and recrystallization of polymer under adiabatic conditions [2–6]. It has some justification since in all tensile drawing and shear experiments massive cavitation and micronecking is involved. In the second, a consideration developed by Young [7,8], invokes the classical theory of crystal plasticity. In that model it is expected that the plastic deformation of polymer crystals, like plastic deformation of crystals of other materials, is crystallographic in nature and takes place without destroying the crystalline order. There are many routes of plastic deformation in which cavitation is suppressed by a compressive stress component, such as processes involving elements of rolling or solid state extrusion. The texture evolution is then a continuous process resulting from interlamellar shear, crystallographic slips and associated crystal rotations [9–11]. Only when cavitation and voiding are present the deformation leads to unravelling the folded chains and break down of the crystals, followed by the formation of a new crystalline structure that may form with no specific crystallographic relationship to the original structure [12,13]. Crystallographic slips are not processes occurring simultaneously over the whole crystallographic plane. In absence of voiding the deformation of polymer crystals is considered to occur

* Corresponding author. Tel.: +48 42 6803250; fax: +48 42 6803261.
E-mail addresses: andgal@bilbo.cbmm.lodz.pl (A. Galeski), argon@mit.edu (A.S. Argon).

0032-3861/$ - see front matter © 2005 Published by Elsevier Ltd.
doi:10.1016/j.polymer.2005.06.073

by dislocation motion within the crystalline lamellae, similar to slip processes observed in metals, ceramics and low-molecular weight crystals. In this plasticity nucleation of dislocations and their motion across slip planes plays a dominant role.

Plastic deformation in crystal plasticity is initiated by yielding of a polymer. Theoretical considerations demonstrated [14] and experiments confirmed [15] that polymer lamellae deform easily by chain slip in the direction of the *c*-axis on specific close-packed planes.

In polymer crystals the generation of dislocations is subject to restrictions. Due to the small thickness of polymer crystals the Frank–Read mechanism of dislocation generation is not possible [16]. Shadrake and Guiu [14] pointed out that in the case of polyethylene the energy necessary for creation of screw dislocations from the edges of lamellae, having Burgers vectors parallel to the chain direction can be supplied by thermal fluctuations in thin crystals.

There are still doubts if this model can apply over a wide range of temperature, from the glass transition of the amorphous component to the onset of melting. The dispute concerns the upper limit of temperature of validity of this approach. Crist [17] suggested that the temperature of γ and α relaxation processes of PE represent the limits of applicability of the model. However, Young [7,8], and Darras and Seguela [18] have used that approach to model the yield behavior of bulk crystallized annealed polyethylene at a much higher temperature.

Seguela [19] proposed that the driving force for the nucleation and propagation of screw dislocations across the crystal width relies on chain twist defects that migrate along the chain stems and allows a step-by-step translation of the stems through the crystal thickness. The motion of such thermally activated defects is responsible for α crystalline relaxation. However, Galeski et al. [9] have shown that in plane strain compression for HDPE at 80 °C the inception of yielding is mainly associated with (100) [001] chain slip within crystalline lamellae. Moreover, it was shown that below the compression ratio of 3.14 only fine slip occurs and is associated with chain tilt and thinning of lamellae. At higher levels of deformation the widespread fragmentation of elongated lamellae, thinned to one third of their initial thickness, takes place. This results because further thinning render the deformation unstable—much like a layered heterogeneous liquid responds by capillary waves and breaks up into stacks of layers.

In many polymers, it was observed that the yield stress increases with increasing thickness of crystals. This relation was studied recently in more detail in polyethylene by Brooks and Mukhtar [20]. Polyethylene has a relatively simple chemical and crystalline structure making it the most widely studied and characterized semi-crystalline polymer [9,11,21]. The procedures applied in the studies of Brooks and Mukhtar [20] allowed obtaining PE orthorhombic crystals with thickness over the range from 3 to 28 nm. An increase of the yield stress with increase of polyethylene crystal thickness was observed for the temperature range from −60 to +60 °C.

Nevertheless, the problem of the dependence of yield behavior on crystal thickness remained still open because the range of thickness of crystal which can be grown is limited by the tendency of all polymers to produce thin lamellar crystals under the common solidification conditions.

We have undertaken the studies of yield behavior of polyethylene with crystals over a much wider range of thickness and have explored the active mechanisms of crystallographic slips by strain rate jump and stress relaxation experiments.

Crystallization of PE under elevated pressure, refined by us [22], makes possible obtaining a number of PE samples with crystal thickness covering the range from the usual 20 nm to nearly chain extended form. The method exploits the pseudo-hexagonal mobile phase of PE at a certain range of pressure and temperature and include both the growth of pseudo-hexagonal domains from the melt that transformed to orthorhombic crystals during cooling and the crystal thickening process by pressurization and heating up to the pseudo-hexagonal phase region without melting. The details for obtaining such a series of samples with crystals of varying thickness under high pressure have been described by us earlier [22].

Most of the previously reported studies of the structural changes caused by deformation were performed in a tensile mode, guided by obvious technological stimuli to explain processes associated with orientation by drawing. However, the deformation by compression is more fundamental as it avoids cavitation and voiding. It was shown [9] that under compression in a channel die no lamellae fragmentation of polyethylene crystals of usual thickness of 10–20 nm occurs up to a compression ratio of three. This is in contrast to serious lamellae fragmentation and destruction occurring in tensile drawing even at low strains. We expect that thick polyethylene crystals will also not show early fragmentation or destruction under compression. Moreover, uniaxial compression has the great advantage because the deformation is nearly a homogenous process and occurs without any significant deformation instabilities such as those observed in tensile drawing where necking can occur. Because of these considerations we have chosen uniaxial compression as the deformation mode in our experiments.

2. Experimental

2.1. Material

High density polyethylene was used in this study: Lupolen 5280HX (BASF) ($M_w = 120{,}000$, $M_w/M_n = 3.4$, density 0.952 g/cm^3 in pellets, MFI of 2.3 at 190 °C/2.16 kg). This experimental grade polymer was supplied by the producer without additives. Additional stabilizers and

antioxidants were added to prevent excessive oxidation of polyethylene during processing and crystallization: A mixture of 0.1 wt% of IRGANOX1010 and 0.2 wt% IRGAFOS168 was dry blended prior to melting and extruding in the form of rods 9.5 mm in diameter. Slightly branched polyethylene (below 5 branches/1000C atoms in the main chain) was chosen for experiments in order to maintain efficient stress transfer between thick crystals with highly extended chains during mechanical tests. Experiments with more linear or lower molecular weight polyethylenes lead also to crystals with the desired thickness range but the samples with thick crystals were found to be brittle, not showing yielding and plastic flow.

2.2. Sample preparation

Fig. 1 shows a schematic of the high pressure cell. The cell is made of ultra high-strength steel (30HGSNA type) capable of withstanding a pressure up to 1000 MPa, at a temperature up to 320 °C. A cylindrical channel is drilled along the axis of the cell, with very high surface smoothness (roughness in the range from 0.02 to 0.12 μm) and high diametral accuracy (max deviation from 0.4 to 0.6 μm). Tungsten carbide rods (hardness of 46/47 HRc which corresponds to hydrostatic pressure within the cylinder of 1650/1680 MPa) tightly matching the diameter and smoothness of the cylindrical opening in the cell are used as plungers. The high accuracy of fitting of the punches to the channel and application of additional brass and Teflon sealings prevent the highly compressed polymer from any leakage out of the cell. Four electrical heaters of 600 W total power, are controlled by a temperature controller, ensuring inside the cell a temperature accuracy of 1 °C. The temperature sensor is placed 10 mm away from the sample in a narrow 1 mm thick channel perpendicular to the wall of the cell. The polymer is compressed by means of an Instron tensile testing machine, via a fixture stabilizing the load exactly along the cell axis. The hydrostatic pressure inside the cell is controlled by means of a tensile testing machine with the accuracy of ± 0.5 MPa. The lower seals were pressed in by the upper plunger without polymer up to the force related to the final desired pressure. Then, after filling the cell with a polymer the upper seals were positioned (between the polymer and copper seal thin Teflon films were placed). The whole system consisting of: lower plunger, lower seals, Teflon, polymer, Teflon, upper seals and upper plunger was loaded up to the desired pressure of the final process. Each time the force was maintained at room temperature for a few minutes to assure that all parts were fitting together in the system. Then, the force was increased to 5.1 kN and the cell was heated up to the temperature of the final process. For samples with crystals in the thickness range around 20 nm the temperature was 200 °C. The polymer was kept in such conditions for 3 min. Then the heaters were switched off and the whole system was cooled down to room temperature and the pressure was released. For the high pressure crystallized samples, after reaching the set temperature (from 210 to 260 °C) the force was raised up to 44.7 kN equivalent to the pressure of 630 MPa. The velocity of the cross head of the tensile testing machine was adjusted (from 0.1 to 5 mm/min), which allowed to control the pressurization rate. Hence, close control of crystallization time at a particular temperature was possible. When a final pressure was achieved the whole system was cooled down to room temperature, and then the pressure was released. Fig. 2 shows a schematic of the procedure where a sketch of the phase diagram of polyethylene is also presented and the course of pressure and temperature paths are marked with arrows.

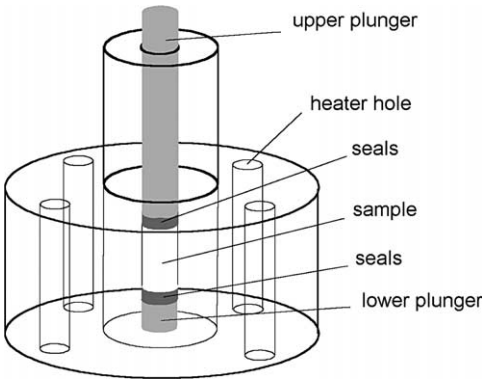

Fig. 1. The scheme of the pressure cell.

Another route for increasing the crystal thickness was thickening without melting. Crystal thickness was increased without melting by pressurization to a desired level, usually to 480 MPa and then heating up to reach the pseudo-hexagonal region of the phase diagram (225 °C), annealed for 30–120 min, cooled down, followed by releasing the pressure. This route is also illustrated schematically in Fig. 2.

Then the samples were pushed out from the cell. Samples, in the form of rods, having 9.5 mm in diameter and about 15 mm in height were partitioned into three 5 mm long cylinders. DSC heating measurements were performed using small portions of the material from both ends of such parts. Abrasive papers with decreasing size of grit were used to grind down the samples to obtain rods having 3 mm

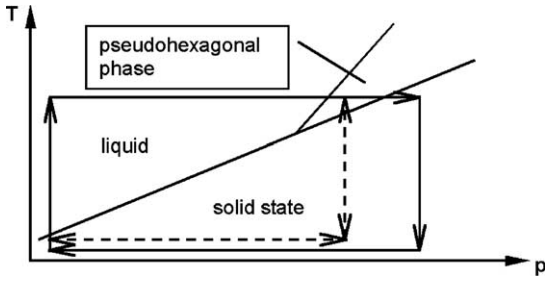

Fig. 2. The sketch of the phase diagram of polyethylene. The routes of crystallization and annealing under pressure are marked.

height and 9.5 mm diameter, appropriate for uniaxial compression.

2.3. Differential scanning calorimetry (DSC)

The thermal analysis of the samples was conducted using an indium-calibrated TA2960 DSC apparatus. Small pieces, of total mass of 4–5 mg, were cut from both ends of 5 mm portions of the rods pushed out from the high pressure cell, placed into aluminium pans and pressed slightly in order to ensure good thermal contact with the DSC cell surface.

The melting thermograms were recorded at a heating rate of 10 °C/min, under nitrogen flow. The crystallinity level and lamellar thickness, l^*, were estimated on the basis of heat of melting of the sample recorded during heating from 60 to 155 °C and from the recorded melting temperature, T_m, respectively. For the determination of l^* the following equation was used [23]:

$$l^* = \frac{2\sigma_e T_m^0}{\Delta h_f (T_m^0 - T_m)} \quad (1)$$

where σ_e is the lamellar basal surface free energy (for PE $\sigma_e = 9\times10^{-6}$ J/cm^2 [24]), Δh_f is the heat of fusion per unit volume (for PE $\Delta h_f = 293$ J/cm^3 [25]), T_m^0 is the extrapolated equilibrium melting temperature measured earlier by us [26] for polyethylene used in this work at 145.1 °C. The set of specimens covering the range from 20 to 170 nm of crystal thickness was obtained by means of crystallization under elevated pressure.

2.4. Mechanical testing

The specimens were uniaxially compressed in order to determine their mechanical properties. The mechanical tests were carried out using an Instron tensile testing machine, sample stabilizing fixture and compression plates. The samples having various crystal thickness were compressed in a special device with initial strain rates of 5.5×10^{-5}, 1.1×10^{-3} and 5.5×10^{-3} s^{-1}. The specimens for compression tests were lubricated on the faces contacting the compression plates of the testing machine to minimize friction.

The yield point is often defined as a stress at a local maximum observed on the load–displacement curve. Such maximum was not observed in our case, because our specimens were tested in uniaxial compression thus avoiding such phenomena like macronecking, micronecking and voiding. Experimentally determined nominal stress–nominal strain curves were corrected to obtain true stress–nominal strain curves. During compression the cross section of the sample increased, the change in cross section was calculated from the change of the height of the specimen assuming no volume change. The following definition of yield point was used: the yield point is at the intersection of measured stress–strain curve and a straight line parallel to initial slope of the curve and offset by 2% of nominal strain.

2.5. Scanning electron microscopy

The bulk morphology of the samples was exposed by cutting the samples with a freshly prepared glass knife. The compressed samples were cut on the circumference of the sample along the compression direction. The exposed surfaces were etched in a solution composed of sulfuric acid and potassium permanganate at room temperature according to the procedure developed originally by Olley et al. [27]. The time of etching was chosen as 30 min based on a series of experiments at room temperature. The samples were carefully washed after etching, dried and then covered with a thin layer of gold by sputtering. The samples were examined in the scanning electron microscope Jeol, 5500LV, working in high vacuum and with accelerating voltage of 10 kV. The micrographs were recorded electronically.

3. Results

A total of 68 samples was prepared differing in crystal thickness and crystallinity. The crystal thickness of obtained samples covers the range from 20 up to 170 nm. The other important parameter, the crystallinity degree was in the range from 60 to 98 wt%.

The morphology of the samples was studied by means of scanning electron microscopy. While the samples obtained under mild pressure and containing thin lamellae exhibit well developed spherulitic morphology, the samples with thicker crystals contain spherulites with ‘rough’ internal structure. The thicker the lamellae the more the roughness of the spherulites. Very thick lamellae are arranged in packets with no spherulite impression. The lamellae packing is illustrated by the typical SEM images of Fig. 3(a)–(c) of a sample containing 100 nm thick crystals and having the crystallinity degree of 91%, as determined from the temperature and heat of melting. Rough disturbed spherulitic structure can be distinguished, in the form of lamellae arranged in differently oriented packets forming a spherulite-like ordering. The thickness of lamellae, as it is measured from SEM image in Fig. 3(a), is roughly 130 nm which agrees fairly with the crystal thickness determined from DSC measurements based on Eq. (1) for this same sample.

Fig. 4(a)–(c) shows representative micrographs of the samples, having initially similar crystal thickness, after compression with the rate of 5.5×10^{-5} s^{-1} to various compression ratios of 1.145, 1.351 and 2.58. Careful scrutiny of the micrographs shows that the initial lamellae thickness was reduced significantly as the compression ratio increased. In Fig. 4(c), the chain stems in lamellae can be clearly identified as a striating pattern on lamellae narrow

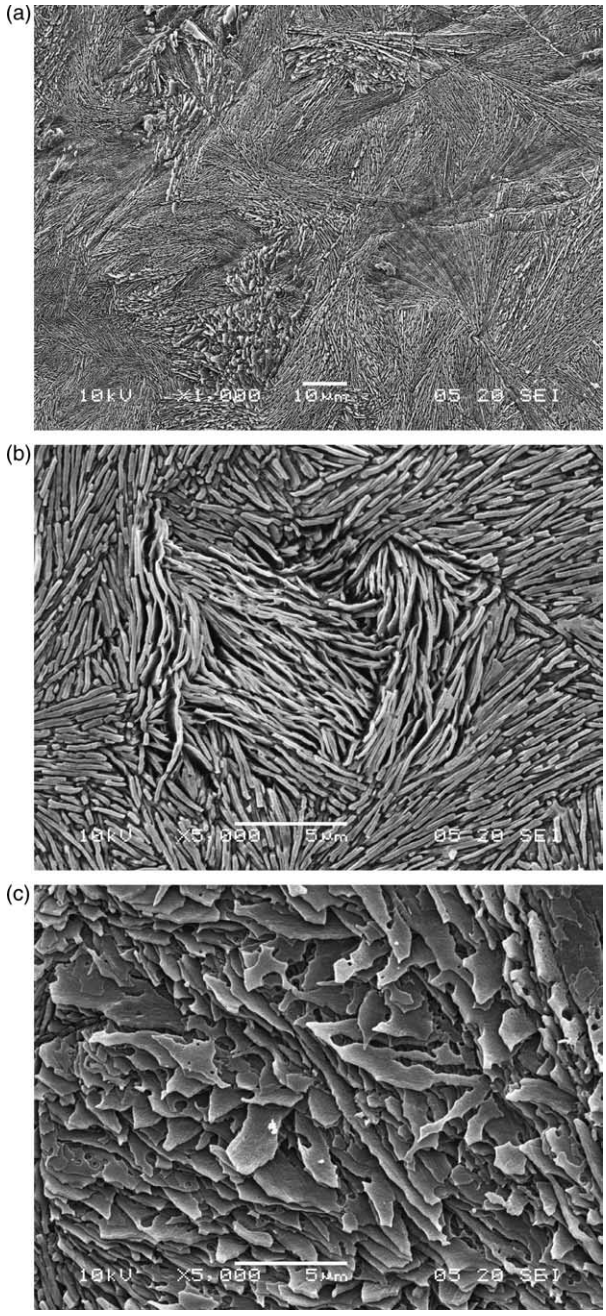

Fig. 3. Scanning electron micrographs of etched surface exposed by sectioning of high density polyethylene sample crystallized by compression of the pressure cell with the rate of 5 mm/min to the pressure of 630 MPa at 250 °C and then cooled down to room temperature. (a) Overview, (b) details showing edge-on lamellae and (c) details showing flat lying lamellae.

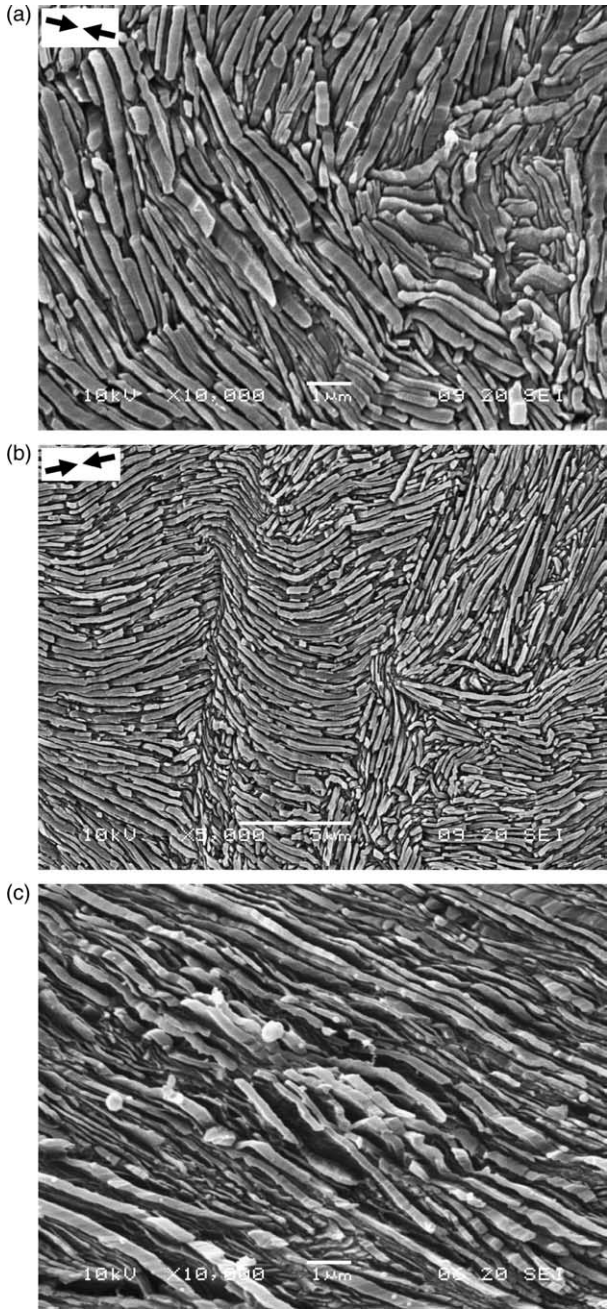

Fig. 4. Scanning electron micrographs of etched surface exposed by sectioning of high density polyethylene samples having similar lamellae thickness (73, 86 and 94 nm) and similar crystallinity (86, 88 and 84%) compressed with the compression rate of $5.5\times10^{-5}\ s^{-1}$ to the increasing compression ratio: (a) 1.145, (b) 1.351 and (c) 2.58.

faces. The striating patterns appear on lamellae narrow faces in the course of etching of deformed lamellae as a result of the presence arrested mobile dislocations. No such striating pattern can be resolved on undeformed lamellae. From Fig. 4(c), it is evident that the chain axes are tilted with respect to the lamellae surfaces and no lamellae fragmentation is observed even for the compression ratio of 2.58. Some other packets of lamellae whose orientation were edge-on during compression underwent kinking at 1–7 μm separation, depending on the initial crystal thickness and the compression ratio (Fig. 5 for an example of kinking and thinning of a polyethylene sample having initially 153 nm thick lamellae, 88% of crystallinity and compressed to a compression ratio of 1.429). Fig. 6(a) and (b) shows the changes due to plastic deformation of two samples having initially similar lamellae thickness subjected to uniaxial compression to a similar compression ratio of 2.6–2.8 with the compression rates differing by two orders of magnitude:

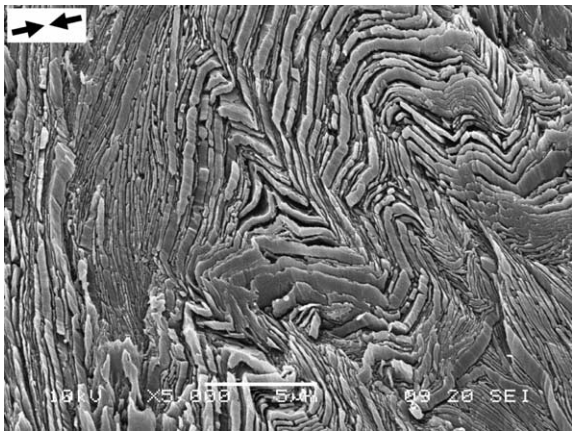

Fig. 5. Kinking and thinning of lamellae, which were initially oriented parallel to the loading direction, due to uniaxial compression with the rate of $5.5\times10^{-5}\,s^{-1}$. Polyethylene sample having initially 153 nm thick lamellae, 88% of crystallinity and a final compression ratio 1.429.

5.5×10^{-5} and $5.5\times10^{-3}\,s^{-1}$. It is seen that both compressed samples show similar features independently of the compression rate: the lamellae became thinner compared with the undeformed samples, chain stems show a tilt with respect to lamellae surfaces and no lamellae fragmentation is observed.

In the literature, the crystallographic slip is documented only for thin PE crystals [15]. No morphological data for the deformation of thicker crystals can be found. From Figs. 3(a)–(c), 4(a)–(c) and 6(a) and (b), it follows that the lamellar crystals undergo shear resulting in their thinning and rotation towards the directions perpendicular to the loading direction. The tilt of stems within lamellae being the result of crystallographic slips is clearly visible. No evidence of lamellae fragmentation can be noticed in the micrographs in all these figures. A small fraction of lamellae, those which were initially aligned parallel to the loading direction, experienced kinking and thinning due to crystallographic slips which is clearly seen in Fig. 5. Other lamellae undergo crystallographic slips and rotation only and no lamellae fragmentation is observed. Other evidence of crystallographic slips and crystal rotation comes from WAXS pole figures of PE samples with increasing compression ratio. Exemplary pole figures for the compression ratio of three are presented in Fig. 7. It is clearly seen that the normals to (200) planes tend to assume the orientation along the loading direction. Since polyethylene crystals are of orthorhombic symmetry, it follows that the (020) normals have a tendency to cluster in the plane of

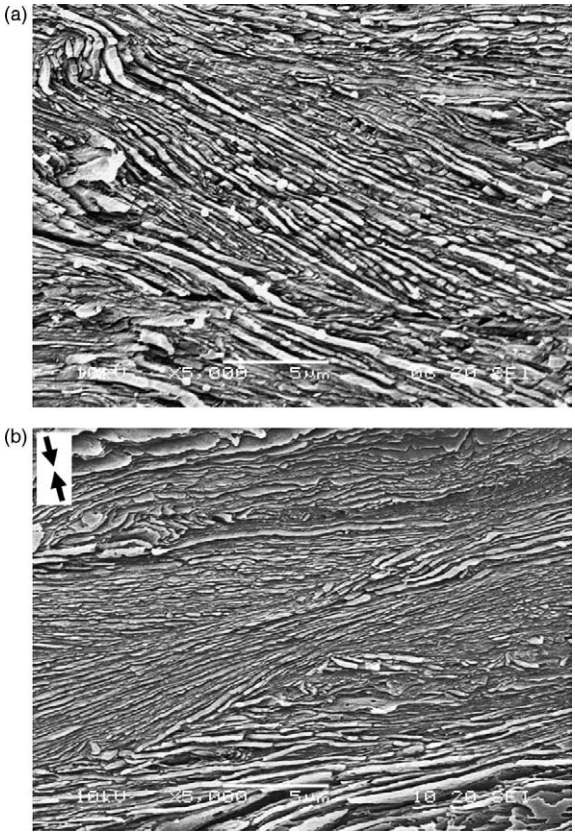

Fig. 6. Scanning electron micrographs of etched surface exposed by sectioning of high density polyethylene samples having similar lamellae thickness (94 and 100 nm), similar crystallinity (84 and 86%) compressed to a similar compression ratio with compression rate differing by two orders of magnitude: (a) $5.5\times10^{-5}\,s^{-1}$ and (b) $5.5\times10^{-3}\,s^{-1}$.

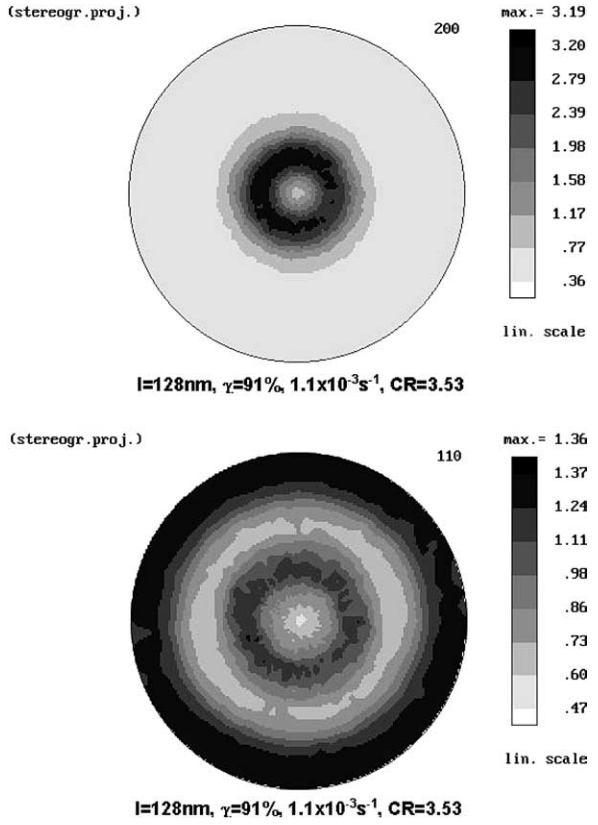

Fig. 7. Exemplary pole figures for (200) and (110) planes of compressed polyethylene samples to a compression ratio of 3.53. The crystallinity and crystal thickness for the samples are depicted in the figure. Projection from the compression direction.

compression. The continuous series of (100) [001] chain crystallographic slips and associated rotations lead to such texture as it was pointed out in one of our earlier papers [9]. Only at higher compression ratio other slip system than (100) [001] become active. The observation of continuous transformation of lamellae by crystallographic slips is also confirmed by the scanning electron micrographs of compressed polyethylene samples in Figs. 3(a)–(c), 4(a)–(c) and 6(a) and (b). It can be concluded then that the observed yielding and plastic flow that follows is always a 'fine slip' process independently of the crystal thickness and there is no discontinuity and no fragmentation of the lamellae during uniaxial compression up to the compression ratio below at least 3.17: Compare Fig. 8 where the scanning electron micrograph of polyethylene sample having 156 nm thick lamellae and degree of crystallinity of 87% compressed to the compression ratio of 3.175 is presented.

Fig. 9(a)–(c) presents three series of true stress–compression ratio curves for polyethylene samples of increasing crystal thickness with various crystallinities for the compression rates of 5.5×10^{-5}, 1.1×10^{-3} and $5.5\times10^{-3}\ s^{-1}$, respectively. It is seen that all the dependencies start with initial elastic response, which is then replaced by yielding. The analysis of the curves delivers a well known conclusions that the yield phenomena does not depend significantly on the crystallinity level, above a certain level assuring the connectivity between crystals via many tie molecules and efficient stress transfer between crystals, in our case above 66%, while it depends considerably on the crystal thickness. The examples for proving the conclusions are the pair of stress–compression ratio curves which do not differ for samples having similar crystal thickness but different crystallinity: The samples with crystal thickness of 85–86 nm differing in crystallinity, 88 vs. 94% (Fig. 9(a)), or the pair of samples with crystal thickness 21–22 nm and crystallinity 70 vs. 75% (Fig. 9(b)). However, the samples having similar crystallinities show markedly different

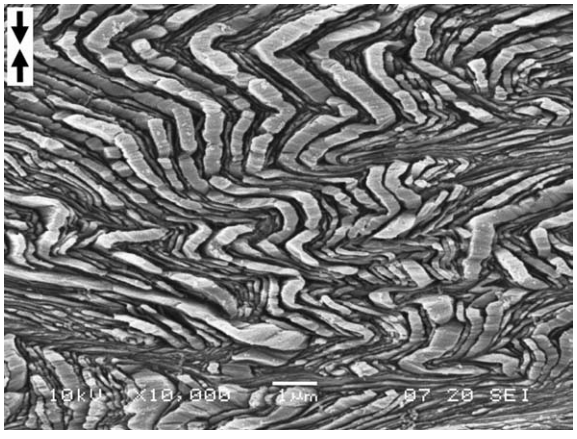

Fig. 8. Scanning electron micrographs of etched surface exposed by sectioning of high density polyethylene samples having 156 nm thick crystals and 87% of crystallinity subjected to compression with the ratio of 3.175. No lamellae fragmentation is observed at such compression ratio.

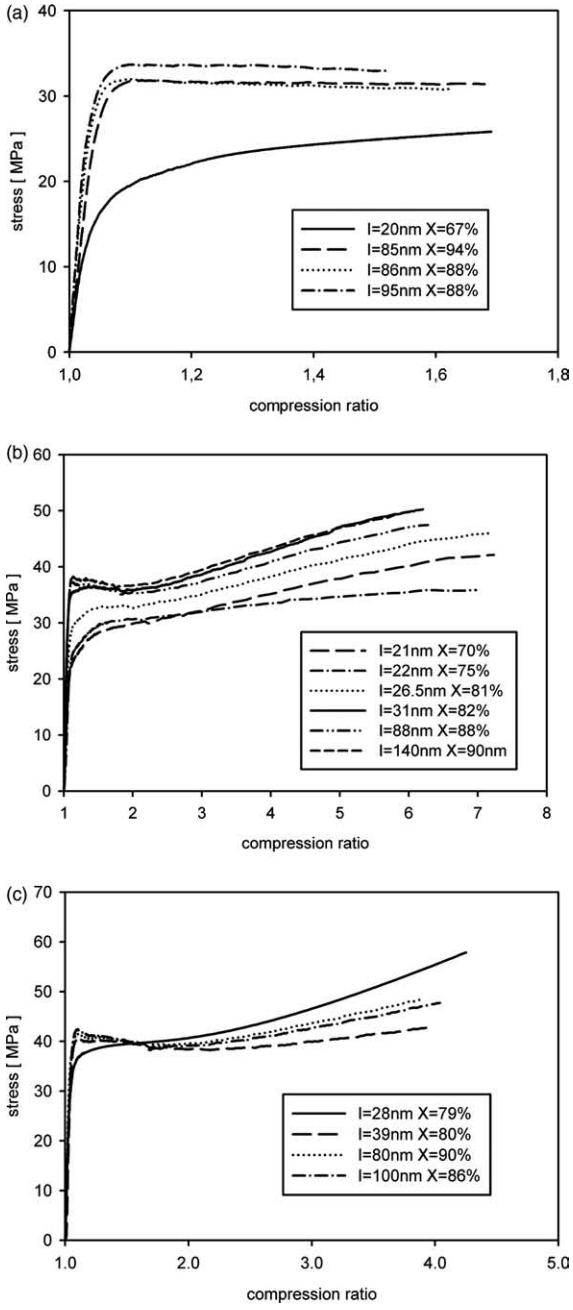

Fig. 9. Four series of exemplary true stress–compression ratio curves for polyethylene samples of increasing crystal thickness with various crystallinities for the compression rates of (a) $5.5\times10^{-5}\ s^{-1}$, (b) $1.1\times10^{-3}\ s^{-1}$ and (c) $5.5\times10^{-3}\ s^{-1}$.

mechanical behavior for different crystal thickness: The pair of samples having 88% of crystallinity and differing in crystal thickness, 86 vs. 95 nm (Fig. 9(a)), the pair of samples having 81–82% crystallinity and differing in crystal thickness, 26.5 vs. 31 nm (Fig. 9(b)) or the pair of samples having 79–80% of crystallinity and differing in crystal thickness, 28 vs. 39 nm (Fig. 9(c)).

For polyethylene samples with thin crystals from Fig. 9(a) and low deformation rate of $5.5\times10^{-5}\ s^{-1}$ the yield sets in at a low stress of slightly above 10 MPa as it can

be seen from Fig. 10(a) where the yield stress of polyethylene samples is plotted against their lamellae thickness. As the crystal thickness increases the yield stress quickly increases: For 30–31 nm thick crystals it approaches 25–28 MPa. Further increase of the crystal thickness produces only a slight increase of the yield stress. The changes in the yield stress with increasing crystal thickness for other initial compression rates of 1.1×10^{-3}, and $5.5\times10^{-3}\,s^{-1}$ are reported in Fig. 10(b) and (c), respectively.

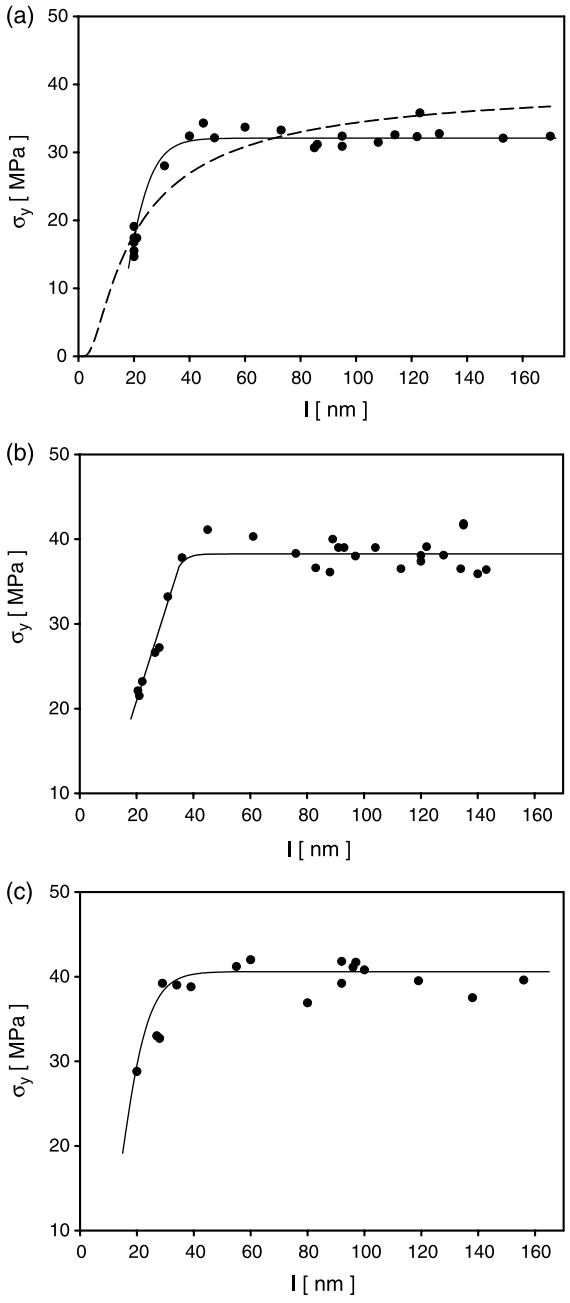

Fig. 10. (a)–(c) The changes in the yield stress with increasing crystal thickness for initial compression rates of (a) $5.5\times10^{-5}\,s^{-1}$, (b) $1.1\times10^{-3}\,s^{-1}$, (c) $5.5\times10^{-3}\,s^{-1}$. The dependence of the yield stress against crystal thickness as expected by the theory of thermally activated mobile dislocations [17] is drawn also in (a).

For all compression rates the yield stress increases initially with crystal thickness up to 40 nm of the crystal thickness and then abruptly saturates. The saturation occurs for crystals thicker than 40 nm independently of the initial compression rate. The yield stress at saturation reaches the level of 32, 37.5, 39.5, 41.0 MPa for initial compression rates of 5.5×10^{-5}, 1.1×10^{-3} and $5.5\times10^{-3}\,s^{-1}$, respectively.

The initial increase of the yield stress with the increase of crystal thickness agrees well with the published results of Brooks and Mukhtar [20] concerning the yield stress of polyethylene in the range of lamellae thickness from 3 to 28 nm. Beyond the region explored in the past by Brooks, some further increase is observed up to the lamellae thickness of 40 nm (Fig.10(a)–(c)). However, above 40 nm of lamellae thickness the yield stress levels off. There is a 'magic' crystal thickness of 40 nm above which the yield saturates independently of the deformation rate.

The initial elastic region extends to the point where no longer further deformation of the amorphous phase is possible. For certain crystal orientation the stress reaches the stress needed for crystal shear and then the yielding sets in. The crystals usually shear along the easiest crystallographic slip plane and in the direction of the easiest slip. The slip occurs when the shear stress resolved in the slip plane exceeds a certain critical value called 'the critical resolved shear stress'. In a homogenous material with no preferred orientation subjected to uniaxial compression the highest shear stress is resolved at 45° with respect to the load. Its value reaches $\sigma \sin 45^\circ \cos 45^\circ = \sigma/2$ where σ is the stress at which the material starts to yield. Hence, the yield stress is a measure of the crystal yield. Polyethylene crystals can yield by the easiest (100) [001] chain slip and at higher deformation ratio the (100) [010] transverse slip system becomes activated [9].

The dependence of the yield stress against crystal thickness as expected by the theory of thermally activated mobile dislocations [7,17] for the following parameters: $T=293K$, effective modulus K at room temperature taken from Karasawa et al. [28] and critical value of the Gibbs free energy $\Delta G_c = 60kT$, are profoundly departing from the experimental data for samples having thick crystals. The curve with a better fit for thick crystals, drawn in Fig. 10(a), uses unrealistic $\Delta G_c = 110kT$. It is then seen that the saturation behavior of the dependence of the yield stress on the crystal thickness is not correctly predicted by that theory.

Any other phenomena such as 'coarse slip' or other spatially limited events which could saturate the yield stress can be eliminated as the reason of leveling off the shear stress because in uniaxial compression such phenomena like micronecking and voiding, which can arise during tensile deformation, are suppressed. In fact it was reported by Bartczak et al. [21] and Galeski et al. [9] that during very similar process of uniaxial compression or plane strain compression of PE no major discontinuities, like

micronecking or lamellar fragmentation were observed up to the compression ratio of 2.5, i.e. far beyond the yield point. Also our careful microscopic examinations reveal only lamellae thinning and rotations up to the compression ratio of 3.175 and no lamellae fragmentation (compare Figs. 3(a) and (b), 4(a)–(c), 6(a) and (b) and 8). Those lamellae which were initially oriented along the loading direction undergo kinking and thinning without fragmentation.

The above observations imply that above 40 nm the crystals thickness is no longer the decisive factor for the yield and that some other mechanism, independent of the crystal thickness, overtakes the control of the yielding process.

According to Young's model of the yield process the yield stress should increase with crystal thickness, which is observed in our experiments but only up to the crystal thickness of 40 nm. The use of thermal analysis of rate dependent processes allows us to measure activation parameters related to crystal plasticity. The kinetic mechanism governing dislocation controlled plasticity can be tested in a strain rate jump experiments [29], where during monotonic deformation, the strain rate $d\gamma_1/dt$ is abruptly increased or decreased to $d\gamma_2/dt$ and the resulting stress jump $\Delta\sigma$ is recorded. The parameter:

$$\Delta\nu^* = \frac{kT}{\Delta\tau}\ln\left[\frac{(d\gamma_1/dt)}{(d\gamma_2/dt)}\right] \quad (2)$$

is the activation volume that characterizes the dependence of the activation free energy on shear stress. In Eq. (2), $\Delta\tau$ must be the shear stress change on the glide system due to the strain rate jump. This is related by factor of 3 to $\Delta\sigma$ which is recorded in an uniaxial experiment. The measurement of $\Delta\nu^*$ allows for classification of material response to strain rate change, and in our case serves to identify the rate controlling mechanisms. We note here that experimentally in an uniaxial straining experiment when a strain rate change is made the change observed is in the uniaxial flow stress $\Delta\sigma$, while the definition of the activation volume must be related to the active shear mechanism and the change $\Delta\tau$ in shear resistance in spherulitic PE, i.e. $\Delta\sigma = 3\Delta\tau$, similar to the relation in a polycrystalline metal [30].

The resulting response of a positive strain rate jump during monotonic deformation for three PE samples having the lamellae thickness of 27, 55 and 96 nm and crystallinity 78, 90 and 87%, respectively, are plotted in Fig. 11 for the initial strain rate of $5.5\times10^{-3}\ s^{-1}$. The positive jump was realized by a sudden change of the strain rate from 5.5×10^{-3} to $5.5\times10^{-2}\ s^{-1}$. The activation volumes determined from these experiments are: 4.71, 6.45 and 7.02 nm^3, respectively. A recognizable yield phenomenon is observed for the samples having the crystal thickness of 55 and 96 nm but only very small one for 27 nm thick crystals. The yield phenomenon corresponds most likely to the dislocation multiplication in these jump experiments. It is often assumed that dislocation generation is immediate and the dislocation density adjusts to a new requirement readily, however, the yield phenomenon observed in a positive strain rate jump suggests otherwise. The existing dislocation density (or source density) is initially preserved and the dislocations are forced to move faster (or sources are required to emit dislocations faster). Soon after a higher dislocation density is established and the flow stress decreases to a lower level in balance with the new strain rate. The yield excess is presented in Table 1.

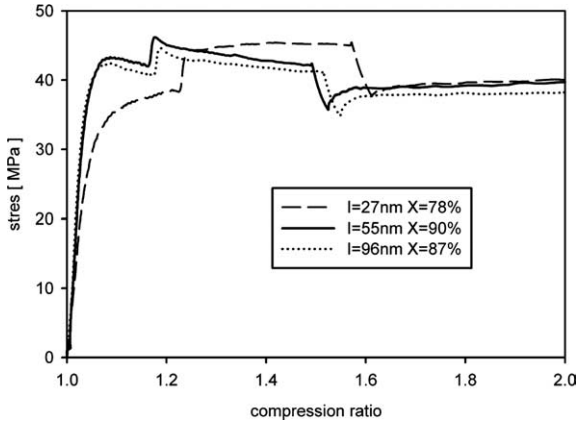

Fig. 11. Strain rate positive and negative jumps for polyethylene sample having the lamellae thickness of 27, 55 and 96 nm and crystallinity 78, 90 and 87%, respectively. The base strain rate is $5.5\times10^{-3}\ s^{-1}$ and jumps were made by one decade increase of the strain rate followed by one decade decrease.

The activation volumes determined from the stresses beyond the yield are the following: 10.11 and 11.88 nm^3, for samples with crystal thickness of 55 and 96 nm, respectively.

The negative jump experiment relied on a sudden strain rate change from 5.5×10^{-2} to $5.5\times10^{-3}\ s^{-1}$. The stress decreases suddenly for all samples, then slowly increases and levels off at a higher value. The stress decrease is caused by the excess concentration of dislocations at higher strain rate. When the excess of mobile dislocations is exhausted a new stress level is reached. The stress increase depends on the crystal thickness and increases with the increase of crystal thickness, first rapidly: By 1.39 MPa for 27 nm thick crystals and to 2.46 MPa for 55 nm thick crystals, and then more slowly to 2.96 MPa for 96 nm thick crystals. The following activation volumes immediately after strain rate drop were obtained: 3.90, 4.11 and 4.47 nm^3, respectively, indicating the low activity of mobile dislocation generation because of their temporary higher concentration shortly after the strain rate drop.

When the stress leveled off the following activation volumes were obtained: 4.92, 6.39 and 8.34 nm^3, respectively. Similar correlations of the activation volumes with crystal thickness were obtained for strain rate jump experiments for samples having crystals with other thicknesses. Those data are collected in Table 1. The following features of the strain rate jump experiments are observed:

Table 1
The activation volumes for strain rate jumps and stress recovery after the negative pressure jump for a series of high density polyethylene samples differing in crystal thickness

Crystal thickness (nm)	Crystallinity (%)	Positive jump			Negative jump			
		Yield overshoot after strain rate (MPa)	Activation volume immediate (nm^3)	Activation volume, at steadiness (nm^3)	Stress recovery after jump (MPa)	Activation volume, immediate (nm^3)	Activation volume, at steadiness (nm^3)	Activation volume from stress relaxation (nm^3)
		Strain rate jumps from 5.5×10^{-3} to 5.5×10^{-2} s^{-1}			Strain rate jumps from 5.5×10^{-2} to 5.5×10^{-3} s^{-1}			
27	78		4.71	4.71	1.39	3.90	4.92	3.36
28	79		4.83	4.83	1.56	3.90	4.95	3.48
29	79		5.04	5.04	1.61	3.66	4.59	3.39
55	90	1.6	6.45	10.11	2.46	4.11	6.39	4.86
92	98	1.51	7.20	11.70	2.77	4.56	8.25	4.89
96	87	1.65	7.02	11.88	2.96	4.47	8.34	4.92
97	86	1.16	6.81	9.45	2.98	4.50	8.55	5.10
		Strain rate jumps from 5.5×10^{-5} to 5.5×10^{-4} s^{-1}			Strain rate jumps from 5.5×10^{-4} to 5.5×10^{-5} s^{-1}			
20	67	Nearly 0	5.67	5.67	0.25	5.88	6.18	8.58
21	70	Nearly 0	5.61	5.61	0.44	6.21	6.87	6.48
20	61	Nearly 0	5.43	5.43	0.72	5.76	5.04	6.48
95	86	0.55	5.16	5.73	0.34	4.71	4.98	8.58
130	92	0.59	6.33	7.29	0.91	5.37	6.21	7.38
170	86	0.6	6.36	7.35	0.72	5.64	6.87	7.77

- in positive strain rate jumps a small yield phenomenon is developed when the sample with thick crystals are deformed and only very small yield phenomenon for thin crystals;
- in negative strain rate jumps the stress decreases suddenly for all samples, then slowly increases and levels off at a slightly higher value;
- the activation volume increases with the increase of crystal thickness. In the strain rate jump experiments from much lower strain rate of 5.5×10^{-5} to 5.5×10^{-4} s^{-1} and from 5.5×10^{-4} to 5.5×10^{-5} s^{-1} for two samples having thin crystals of 20 nm and thick crystals 95 nm similar phenomena are observed as for two orders of magnitude faster strain rates.

The activation volume data for these low strain rate jump experiments are collected at the bottom of Table 1.

The stress relaxation, when the deformation is stopped, usually follows the logarithmic variation with time. The change in stress is described by the formula:

$$\Delta\tau = -\left(\frac{kT}{V_r}\right)\ln\left(1+\frac{t}{c_r}\right) \tag{3}$$

which can be transformed by differentiation to:

$$V_r = kT\left[\frac{\partial \ln(d\gamma/dt)}{\partial\tau}\right] = 3kT\left(\frac{\partial \ln \dot{\varepsilon}}{\partial\sigma}\right) \tag{4}$$

where c_r is a time constant and V_r has the dimension of a volume and a physical meaning of apparent activation volume during stress relaxation, $\dot{\varepsilon}$ and σ refer to the uniaxial strain rate and uniaxial stress while $\dot{\gamma}$ and τ to the shear strain rate and shear stress at the mechanisms level [30]. Hence, the material relaxing logarithmically yields the following parameters: A time constant c_r and apparent activation volume V_r. In fact all our systems were relaxing in that way which is shown in Fig. 12 where the exemplary dependence $\ln(\Delta\sigma/\Delta t)$ vs. $\Delta\sigma_-$ assumes a straight line. The activation volumes from the stress relaxation experiments are collected in the last column of Table 1. These values increase abruptly with the increase of the crystal thickness from 3.36 to 3.48 nm^3 and saturate for thicker crystals at approximately 5.10 nm^3.

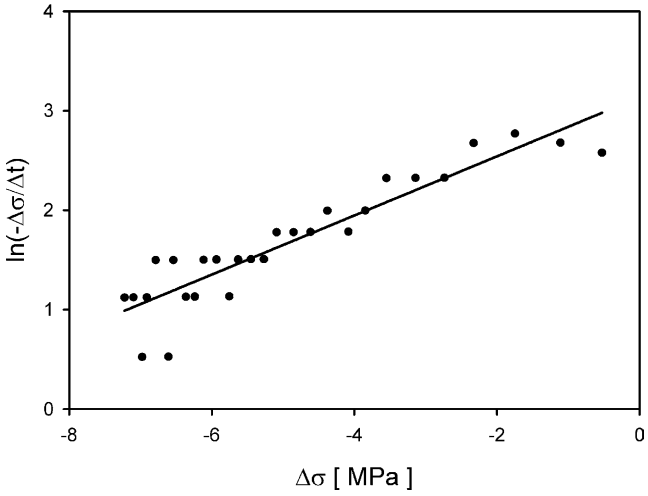

Fig. 12. Relaxation of a compressive stress expressed in the Eyring coordinates for a polyethylene sample having average lamellae thickness of 29 nm and crystallinity of 80%. The initial comlpression rate was 0.055 s^{-1}.

4. Discussion and conclusions

Samples with a broad range of crystals thickness (from usual 20 up to 170 nm) were obtained under high pressure annealing in the region of temperature and pressure characterized by pseudo-hexagonal packing of PE. This region was reached either via pressurization and then heating (without melting) or via heating and then pressurization (with melting). Crystal thickness depends on temperature, pressure and annealing time in the pseudo-hexagonal region. Independently of crystallinity and crystal thickness the samples underwent recoverable compression up to the compression ratio of approximately 1.05–1.07. Then the yield was reached and plastic flow set in above the compression ratio of 1.12. At a compression rate of $5.5\times10^{-5}\,s^{-1}$ for thin crystals the yield stress increases with the increase of crystal thickness from 15–20 MPa for 20–30 nm thick crystals to 28–30 MPa for 40 nm thick crystals. Further increase of crystal thickness, even up to 170 nm thick, does not cause any marked increase of the yield stress. In the range of crystallinities exhibited by the samples, above 60 wt%, the yield stress does not depend significantly on the crystallinity level and is determined by the crystal thickness. Uniaxial compression with a higher rate increases the yield stress, however, the mechanism of the yield stress increase due to the increase of crystal thickness is only effective up to the thickness of 40 nm. For the compression rate of $5.5\times10^{-3}\,s^{-1}$ the yield stress reaches 41 MPa for thick crystals. The experimental dependence of the yield stress vs. crystal thickness was compared with a model developed on the basis of classical crystal plasticity [14] and nucleation of screw dislocations [7]. The yield stress displays the dependence on strain rate, which is expected in crystal plasticity as in Young's model. With the increase of crystal thickness the yield stress increases up to 28–30 MPa for 40 nm thick crystals exactly as predicted is by the Young theory for thermally assisted dislocation generation. However, in contrast to that model the yield stress saturates with the increase of crystal thickness above 40 nm.

The activation volumes obtained from strain rate jumps are around 4.5–4.8 nm^3 for both negative and positive jumps which corresponds to about 18 nm^2 considering the Burgers vector for orthorhombic crystals of polyethylene at 0.253 nm.

Above 40 nm, the dependence of the yield stress on crystal thickness quickly levels off. This indicates that for thick lamellae the mechanism of screw dislocation emission from edges of lamellae becomes too difficult and another mechanism must take over that is independent of the thickness of the lamellae. In a companion paper, we propose that this mechanism consists of nucleation of edge and screw dislocation half loops from the large and small faces of the lamellae, respectively. This mechanism not only explains the transition from a flow stress rising with increasing thicknesses of lamellae to a flow stress independent of lamellae thickness but also explains better the temperature dependence of the flow stress of crystals having usual 10–20 nm thickness and gives a much better understanding of the levels of activation volume reported here [31].

Acknowledgements

PhD Grant KBN 7 T08E 017 21 (for T. Kazmierczak) and Grant KBN 7 T08E 055 22 both from the State Committee for Scientific Research (Poland) are acknowledged for the financial support. A.S.A. acknowledges support of the Mechanical Engineering Department at M.I.T. Authors are grateful to Dr M. Slouf from Institute of Macromolecular Chemistry, Czech Acad. Sci., Prague, for assistance in SEM.

References

[1] Galeski A. Prog Polym Sci 2003;28:1643–99.
[2] Flory PJ, Yoon DY. Nature 1978;272:226–9.
[3] Tuo-Min L, Juska TD, Harrison IR. Polymer 1986;27:247–9.
[4] Juska T, Harrison IR. Polym Eng Sci 1982;22:766–76.
[5] Popli R, Mandelkern L. J Polym Sci, Polym Phys Ed 1987;24:441–83.
[6] Gent AN, Madan S. J Polym Sci, Polym Phys Ed 1989;27:1529–42.
[7] Young RJ. Philos Mag 1976;30:86–94.
[8] Young RJ. Mater Forum 1988;11:210–6.
[9] Galeski A, Bartczak Z, Argon AS, Cohen RE. Macromolecules 1992; 25:5705–18.
[10] Lin L, Argon AS. J Mater Sci 1994;29:294–323.
[11] Bartczak Z, Cohen RE, Argon AS. Macromolecules 1992;25: 4692–704.
[12] Annis BK, Strizak J, Wignall GD, Alamo RG, Mandelkern L. Polymer 1996;37:137–40.
[13] Peterlin A. J Macromol Sci, Phys 1971;6:490–508.
[14] Shadrake LG, Guiu F. Philos Mag 1974;34:565–81.
[15] Bowden PB, Young RJ. Nature 1971;229:23–5.
[16] Frank FC, Read WT. Phys Rev 1950;79:722–3.
[17] Crist B. Polym Commun 1989;30:69–71.
[18] Darras O, Seguela R. J Polym Sci, Part B: Polym Phys 1993;31:759–66.
[19] Seguela R. J Polym Sci, Part B: Polym Phys 2002;40:593–601.
[20] Brooks NWJ, Mukhtar M. Polymer 2000;41:1475–80.
[21] Bartczak Z, Argon AS, Cohen RE. Macromolecules 1992;25:5036–53.
[22] Kazmierczak T, Galeski A. J Appl Polym Sci 2002;86:1337–50.
[23] Hoffman JD. Polymer 1983;24:3–26.
[24] Hoffman JD. Polymer 1982;23:656–70.
[25] Wunderlich B, Czornyj G. Macromolecules 1977;10:906–13.
[26] Psarski M, Piorkowska E, Galeski A. Macromolecules 2000;33:916–32.
[27] Olley RH, Hodge AM, Basset DC, Thomson JJ. J Polym Sci, Polym Phys 1979;17:627–43.
[28] Karasawa N, Dasgupta S, Goddard W. J Phys Chem 1991;95:2260–72.
[29] Lin L, Argon AS. Macromolecules 1994;27:6903–14.
[30] Lee BJ, Argon AS, Parks DM, Ahzi S, Bartczak Z. Polymer 1993;34: 3555–75.
[31] Argon AS, Galeski A, Kazmierczak T. Submitted for publication.